

# CNN as Curve Shortening Flow Computer

*István Petrás, Tamás Roska*

Analogic and Neural Computing Systems Laboratory, Computer  
and Automation Research Institute of the Hungarian Academy  
of Sciences, Kende u.11, Budapest, 1111 - Hungary

petras@sztaki.hu

**ABSTRACT:** The CNN as a curve shortening flow PDE computer is introduced. It is shown that the state derivative of the CNN is the quasi-linear function of the local curvature of the evolving shape. Experiments demonstrated that the hardware feasible CNN is suitable wave computer for morphological scale-space processing of shapes.

## 1. Introduction

The CNN [1-2] as an active media has been studied extensively. Several types of nonlinear waves has been reproduced and analyzed on this structure depending on the complexity of the elementary cells [3][5]. Recently many paper dealt with the CNN as a wave-computing device [4]–[7]. It has been proved to be a suitable computing frame for wave based image processing. Some of these algorithms used autowaves for specific task [8] others used trigger waves for some kind of morphological processing in which the shape is deformed by the wave. These trigger wave-based processes were unidirectional i.e. if the spreading wave triggered a cell then it remained triggered [6]. However using an appropriate nonlinear diffusion operator this property can be violated yielding a qualitatively different behavior [9]. The phenomenon that is well known from the image processing literature is described by

$$\frac{\partial C(l, t)}{\partial t} = -\kappa \vec{N} \quad (1)$$

where  $C$  is the boundary vector of coordinates (the curve),  $\vec{N}$  is the outward normal,  $l$  is the curve parameter,  $t$  is the scale parameter. This equation is known as the geometric heat equation or curve shortening flow in differential geometry. Several work dealt with this flow (see for review e.g. [16]). It had been proved [10] that all closed contour collapses into a single point under this flow. During the evolution the shape (closed contour) collapses under its curvature that give rise to obtain a hierarchy of shapes and thus a scale space for shapes is formed [11][12]. These scale spaces gave a suitable framework for recognition, classification and retrieval of shapes. Due to numerical and theoretical reasons Osher and Sethian proposed an approach in which the curve flow is embedded into a level set evolution of a surface [13]. This surface is evolved by its mean curvature. It was proved that the zero level set evolves according to the original curve flow.

The CNN based nonlinear diffusion works similar way. The shape is given as the initial state of the array. The zero level set (or iso-intensity line) of the state is considered as the evolving contour of the shape during the evolution (see Fig. 1). Black (+1) color means “inside” white means “outside” of the shape. Using the discretized version of the following reaction-diffusion operator  $A(\cdot) = D\nabla^2 f(\cdot) + a f(\cdot)$  the CNN computes the approximation of curve shortening flow in one transient.

At the beginning of the evolution of the CNN the shape is implicitly embedded into a surface through the blurring of the diffusion process. As a result a linear transition zone is formed between the black and white regions. Cells belonging to the zone are in the linear region of (5). Cells being black or white are said to be saturated. They are in the saturation region of (5). The width of the linear region can be influenced by parameters  $D$  and  $a_e$ . However the blur is spatially limited: the nonlinear character of the diffusion maintains the constant width and the gradient of the linear zone. This width is independent of the orientation and of the shape of the zone throughout the transient. When the desired curve smoothing is reached the transient is stopped. The CNN can be used as an effective parallel “curve shortening flow computer” and we can use the theories developed for scale-spaces for shape ([11][12]).


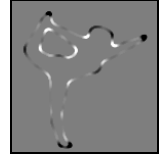



Output					
time	original shape	local curvature at t=1	t= 4	t=14	t=34

Figure 1 Evolution of a shape according to its local curvature.  $s=0.6, p=-1$ , the boundary is zeroflux

## 2. The state derivative and the curvature

In the following we present validation of the relation between the local curvature of the edge contour of the evolving shape and the dynamics of the CNN. Let the CNN be:

$$\dot{x}_{ij}(t) = -x_{ij}(t) + \sum_{k=-r}^r \sum_{l=-r}^r A_{kl} f(x_{i+k, j+l}(t)) \quad \mathbf{A} = \begin{bmatrix} 0 & s & 0 \\ s & p & s \\ 0 & s & 0 \end{bmatrix} \quad (2)$$

where  $s>0, p<1, 4s+p-1>0, f$  is same as (5). Let  $s=D/4, p=a_e-D$

### Proposition:

The temporal derivative of the state variable of a linear cell being in the boundary region is the quasi-linear function of the local curvature of the iso-intensity line to which the cell belong provided that the gray level of the cell is close to zero and that the number of linear cells is greater or equal than 3.

$$\dot{x}_{ij} = F(\kappa), \quad \text{where } \kappa \text{ is the local curvature} \quad (3)$$

### Validation:

Let us suppose that a qualitatively equivalent PDE representation exist of the autonomous CNN of eq. (2). Let us denote  $u = u(x, y, t), u \in \mathbf{R}^2 \times \mathbf{Z} \rightarrow \mathbf{R}$

$$\frac{\partial u}{\partial t} = -u + D \nabla^2 f(u) + a_e f(u), \quad \text{where } D=s, a_e=p+4s \text{ is constant} \quad (4)$$

Let  $f = \lim_{\varepsilon \rightarrow 0} f_\varepsilon$  is as in (5) [15]:

$$f_\varepsilon(x) = \begin{cases} -1 & x \leq -(1+\varepsilon) \\ \frac{1}{4\varepsilon}[x^2 + 2(1+\varepsilon)x + (1-\varepsilon)^2] & |x+1| \leq \varepsilon \\ x & |x| \leq 1-\varepsilon \\ -\frac{1}{4\varepsilon}[x^2 - 2(1+\varepsilon)x + (1-\varepsilon)^2] & |x-1| \leq \varepsilon \\ 1 & x \geq 1+\varepsilon \end{cases} \quad f'_\varepsilon(x) = \begin{cases} 0 & x \leq -(1+\varepsilon) \\ \frac{1}{2\varepsilon}[x+(1+\varepsilon)] & |x+1| \leq \varepsilon \\ 1 & |x| \leq 1-\varepsilon \\ -\frac{1}{2\varepsilon}[x-(1+\varepsilon)] & |x-1| \leq \varepsilon \\ 0 & x \geq 1+\varepsilon \end{cases} \quad f''_\varepsilon(x) = \begin{cases} 0 & x \leq -(1+\varepsilon) \\ \frac{1}{2\varepsilon} & |x+1| \leq \varepsilon \\ 0 & |x| \leq 1-\varepsilon \\ -\frac{1}{2\varepsilon} & |x-1| \leq \varepsilon \\ 0 & x \geq 1+\varepsilon \end{cases} \quad (5)$$

Let us expand  $\nabla^2 f(u)$ :  $\nabla^2 f(u) = \frac{\partial}{\partial x} \left( \frac{\partial f}{\partial u} \frac{\partial u}{\partial x} \right) + \frac{\partial}{\partial y} \left( \frac{\partial f}{\partial u} \frac{\partial u}{\partial y} \right) = f''(u) (\|\nabla u\|^2) + f'(u) \nabla^2 u$  (6)

Substituting (6) into (4) we get:

$$\frac{\partial u}{\partial t} = -u + D \left( f''(u) \|\nabla u\|^2 + f'(u) \nabla^2 u \right) + a_e f(u) \quad (7)$$

Observe that we have now two terms inside of the parenthesis: the first one is the product of the square of the vector norm of the gradient and of the second derivative of the nonlinearity. The second term is the product of the derivative of the nonlinearity and of the Laplacian of  $u$ . Using notation  $u_\eta = \partial u / \partial \eta$ ,  $u_{\eta\eta} = \partial^2 u / \partial \eta^2$  the Laplace operator can be written as [16]:

$$\nabla^2 u = u_{\xi\xi} + u_{\eta\eta} = u_{\eta\eta} + \kappa u_\eta. \quad (8)$$

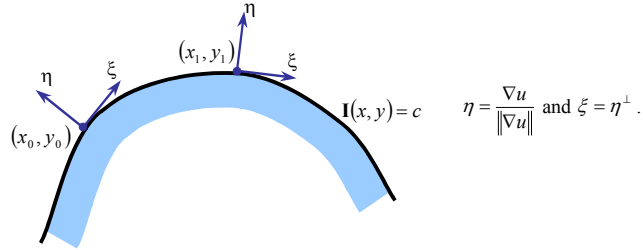


Figure 2 The definition of the moving local coordinate system along the image contour.

This curvature  $\kappa$  is the same for the surface  $u$  and for the embedded curve at the zero iso-intensity level. This is because of  $u$  has a linear shape around the zero level set ( $u_{\eta\eta} \approx 0$ ). We know that

$$\|\nabla u\|^2 = u_x^2 + u_y^2 = u_\eta^2, \quad (9)$$

where  $u_x, u_y$  denotes the derivative along the  $x$  axis,  $y$  axis respectively. Substituting eq. (8) into (7) and using (9) we get the following one-dimensional equation:

$$\frac{\partial u}{\partial t} = -u + D \left( f''(u) u_\eta^2 + f'(u) (u_{\eta\eta} + \kappa u_\eta) \right) + a_e f(u). \quad (10)$$

Now we see that the behavior of the PDE depends on the local curvature  $\kappa$ . Inside of the linear region the influence of the curvature is dominant. Close to the edges of the linear region the importance of the curvature decreases while the square of the gradient determines the state derivative. Let us now suppose that  $u$  is in the linear region of the nonlinearity. Inside of this region ( $|u| \leq 1-\varepsilon$ )  $f''(u) = 0$  and  $f'(u) = 1$ . Using this we get

$$\frac{\partial u}{\partial t} = -u + D(u_{\eta\eta} + \kappa u_{\eta}) + a_e u. \quad (11)$$

Let consider the case when  $u$  is zero which means it is on the zero iso-intensity line. Thus we can write:

$$\frac{\partial u}{\partial t} = Du_{\eta\eta} + D\kappa u_{\eta} \approx D\kappa u_{\eta}, \quad \text{where } u_{\eta} < 0 \text{ always.} \quad (12)$$

The speed of a point on the iso-intensity line along the gradient can be computed  $\partial\eta/\partial t = (\partial u/\partial t)/(\partial u/\partial\eta)$ , thus we get  $\partial\eta/\partial t = Du_{\eta\eta}/u_{\eta} + D\kappa$ . In this equation  $|u_{\eta\eta}/u_{\eta}| \ll 1$  is a small number. As a result we see that the curve is moving according to the local curvature since  $\eta$  is the basis vector of our local coordinate system along the gradient:

$$\frac{\partial\eta}{\partial t} = D\kappa. \quad (13)$$

The curvature of the surface  $u$  and the embedded curve are the same when  $u$  is on the zero iso-intensity line. Of course relation (12) is valid only in the linear region of the CNN.

*From PDE to CNN*

To obtain the CNN representation we make the spatial discretisation of (11) with  $h=1$ ,  $(\cdot)_{\eta} = [-1/2 \ 0 \ 1/2]$ ,  $(\cdot)_{\eta\eta} = [1 \ -2 \ 1]$ :

$$\frac{dx_i}{dt} = -x_i + \frac{D}{4} \left( x_{i-1} - 2x_i + x_{i+1} + \frac{1}{2} (\kappa x_{i-1} - \kappa x_{i+1}) \right) + a_e x_i. \quad (14)$$

Let  $a_e = p+4s$  and  $D = 4s$ . Substituting this into (14) we get

$$\frac{dx_i}{dt} = -x_i + s \left( 1 + \frac{\kappa}{2} \right) x_{i-1} + (p+2s)x_i + s \left( 1 - \frac{\kappa}{2} \right) x_{i+1}. \quad (15)$$

In the following let us investigate the effect of  $\kappa$ .

**Case 1.** If  $\kappa = 0$  equation (15) is the same as equation (6) in [14] in the linear region:

$$\frac{dx_i}{dt} = -x_i + \hat{s}^+ x_{i-1} + \hat{p} x_i + \hat{s}^- x_{i+1}. \quad (16)$$

where  $\hat{p} = p+2s$  and  $\hat{s}^+ = \hat{s}^- = s$ . Thus theorems and results developed in that case can be used too.

**Case 2.** If  $\kappa \neq 0$  then from equation (16)

$$A = \left[ s \left( 1 + \frac{\kappa}{2} \right) \quad p+2s \quad s \left( 1 - \frac{\kappa}{2} \right) \right] \quad (17)$$

If the curvature is zero then the 2D problem is reduced into orientation independent 1D problem and stability results [14] developed in the 1D case are valid. Moreover, the result strongly conjectures that if the curvature is not zero the contour region will move according to the sign and value of the curvature. Experiments support well the conjecture.

### 3. Examples

**Disc deformation.** In this experiment we measured the change of state derivative  $x$  of the CNN during the evolution. The initial state was a black disc. During the transient the disc was continuously shrinking with increasing speed until it disappeared. Meanwhile, the average magnitude of the state derivative in the linear transition zone got greater and greater. At the same time the real curvature of the disc was computed according to the relation  $\kappa = 1/R_t$ , where  $R_t$  is the actual radius of the disc. Results are shown in Fig. 3 and Fig. 4.

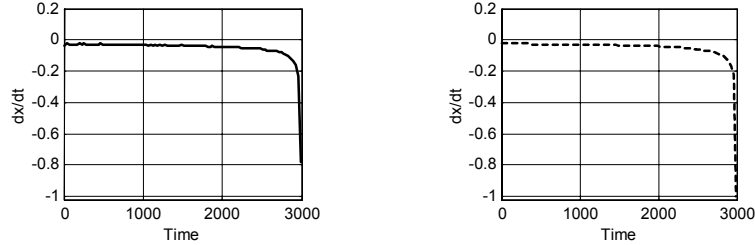


Figure 3 The real curvature of the disc  $= 1/R_t$  (solid line) and the state derivative of the CNN (dashed line). ( $p=-1.25, s=0.6, r=0$ )

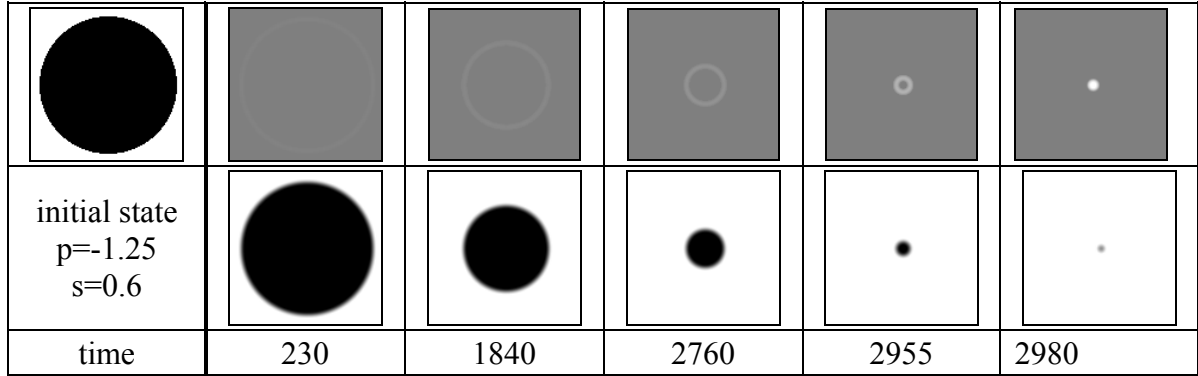


Figure 4 Measurement of the curvature. The first row contains the state derivative. The gray level encodes the curvature. White means negative curvature. ( $p=-1.25, s=0.6, r=0$ , image size:  $128 \times 128$ )

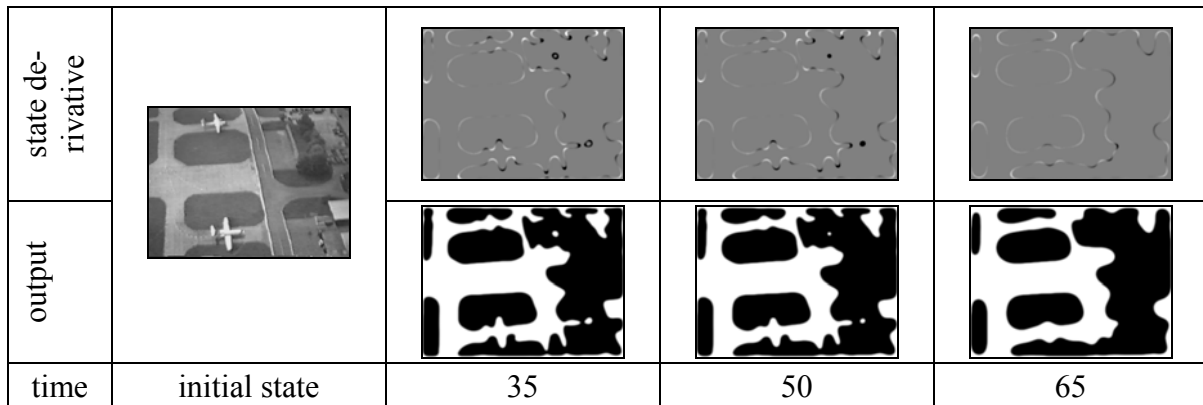


Figure 5 Curvature smoothing in complex scene. Upper row shows the snapshots of the state derivative. The bottom row shows the output of the CNN. ( $p=-1.1, s=0.6, r=0$ , image size:  $320 \times 240$ )

**Complex shape deformation.** In this experiment simulation shows the evolution of the shapes of an airport scene. Snapshots in Fig. 5 show that the contours are smoothed; however the shape is continuously distorted meanwhile. Observe that small-scaled structures disappear as the system evolves. The gray level shows the magnitude and the sign of the curvature. This makes it possible to use it as basic building block of complex feature detection algorithms.

#### 4. References

- [1] L. O. Chua and L. Yang, "Cellular Neural Networks: Theory and Applications", IEEE Trans. on Circuits and Syst., Vol. 35, pp. 1257-1290, Oct. 1988.
- [2] T. Roska and L. O. Chua, "The CNN Universal Machine: an Analogic Array Computer", IEEE Trans. on Circuits and Systems, Vol. 40, pp. 163-173, March 1993.
- [3] L. O. Chua, Ed., "Special Issue on Nonlinear Waves, Patterns and Spatio-Temporal Chaos in Dynamic Arrays," IEEE Transactions on Circuits and Systems: I, vol. 42, no. 10, Oct. 1995.
- [4] Á. Zárandy, R. Domínguez-Castro, S. Espejo "Ultra-high frame rate focal plane image sensor and processor", IEEE Sensor Journal, December 2002
- [5] I. Petrás, C. Rekeczky, T. Roska, R. Carmona, F. Jimenez-Garrido, and A. Rodriguez-Vazquez, "Exploration of Spatial-Temporal Dynamic Phenomena in a 32×32-Cells Stored Program 2-Layer CNN Universal Machine Chip Prototype", Journal of Circuits, Systems, and Comp. (JCSC) Vol. 12, No. 6, 2003
- [6] C. Rekeczky and L. O. Chua, "Computing with Front Propagation: Active Contour and Skeleton Models in Continuous-Time CNN," Journal of VLSI Signal Processing Special Issue: Spatio-temporal Signal Processing with Analogic CNN Visual Microprocessors, vol. 23, 1999, pp. 373-402.
- [7] I. Szatmári, A. Schultz, C. Rekeczky, T. Kozek, T. Roska and L. O. Chua, "Bubble-Debris Classification via Binary Morphology and Autowave Metric on CNN," IEEE Trans. on Neural Networks, vol. 11, 2000, pp. 1385-1393.
- [8] P. Arena, A. Basile, L. Mattia, "CNN Wave Based Computation for Robot Navigation Planning," Proc. of ISCAS 2004, 2004
- [9] I. Petrás, T. Roska, "Application of Direction Constrained and Bipolar Waves for Pattern Recognition," CNNA2000, Proc., pp. 3-8, Catania, Italy, 2000
- [10] M. A. Grayson "The heat equation shrinks embedded plane curves to round points," J. Diff. Geom., vol. 29, pp. 285-314, 1987.
- [11] F. Mokhtarian, A. Mackworth, "A Theory of Multiscale, Curvature-Based Shape Representation for Planar Curves," IEEE PAMI, Vol. 14, No. 8, pp. 789-805, 1992
- [12] B. Kimia, A. Tannenbaum, and S. Zucker, "Shape, shocks, and deformations I: The components of two-dimensional shape and the reaction-diffusion space," Intern. Journal of Comp. Vision, Vol. 15, pp. 189-224, 1995.
- [13] S. Osher, and J. A. Sethian, "Fronts Propagating with Curvature Dependent Speed: Algorithms Based on Hamilton-Jacobi Formulation", Journal of Computational Physics, Vol. 79, pp. 12-49, 1988.
- [14] P. Thiran, K. R. Crouse, L. O. Chua, and M. Hasler, "Pattern formation properties of autonomous cellular neural networks", IEEE Trans. Circuits Syst. I, vol. 42, pp. 757-774, Oct. 1995.
- [15] M. Biey, P. Checco, and M. Gilli, "Bifurcation and chaos in CNNs", Journal of Circuits Systems and Computers, vol. 12, no. 4, pp. 417-433, August 2003.
- [16] B.M.H. Romeny (ed.), Geometry-driven Diffusion in Computer Vision, Kluwer Academic Publishers, pp. 49, 1994.